Nanoscale Res Lett (2010) 5:1603–1610
DOI 10.1007/s11671-010-9683-1

NANO EXPRESS

Nanostructured Systems Containing Rutin: In Vitro Antioxidant Activity and Photostability Studies

Juliana S. Almeida · Fernanda Lima · Simoní Da Ros · Luis O. S. Bulhões · Leandro M. de Carvalho · Ruy C. R. Beck

Received: 7 May 2010 / Accepted: 30 June 2010 / Published online: 15 July 2010

Abstract The improvement of the rutin photostability and its prolonged in vitro antioxidant activity were studied by means of its association with nanostructured aqueous dispersions. Rutin-loaded nanocapsules and rutin-loaded nanoemulsion showed mean particle size of 124.30 ± 2.06 and 124.17 ± 1.79, respectively, polydispersity index below 0.20, negative zeta potential, and encapsulation efficiency close to 100%. The in vitro antioxidant activity was evaluated by the formation of free radical ·OH after the exposure of hydrogen peroxide to a UV irradiation system. Rutin-loaded nanostructures showed lower rutin decay rates [$(6.1 \pm 0.6)\ 10^{-3}$ and $(5.1 \pm 0.4)\ 10^{-3}$ for nanocapsules and nanoemulsion, respectively] compared to the ethanolic solution [$(35.0 \pm 3.7)\ 10^{-3}\ min^{-1}$] and exposed solution [$(40.1 \pm 1.7)\ 10^{-3}\ min^{-1}$] as well as compared to exposed nanostructured dispersions [$(19.5 \pm 0.5)\ 10^{-3}$ and $(26.6 \pm 2.6)\ 10^{-3}$, for nanocapsules and nanoemulsion, respectively]. The presence of the polymeric layer in nanocapsules was fundamental to obtain a prolonged antioxidant activity, even if the mathematical modeling of the in vitro release profiles showed high adsorption of rutin to the particle/droplet surface for both formulations. Rutin-loaded nanostructures represent alternatives to the development of innovative nanomedicines.

Keywords Antioxidant activity · Nanocapsules · Nanoemulsions · Nanoparticles · Photostability · Rutin

J. S. Almeida · L. M. de Carvalho
Programa de Pós-Graduação em Ciências Farmacêuticas, Universidade Federal de Santa Maria, Av. Roraima, 1000, Santa Maria, RS 97105-900, Brazil

F. Lima · S. D. Ros · L. M. de Carvalho
Departamento de Química, Universidade Federal de Santa Maria, Santa Maria, RS 97105-900, Brazil

L. O. S. Bulhões
Departamento de Química, Universidade Federal de São Carlos, São Carlos, SP 13565-905, Brazil

R. C. R. Beck (✉)
Faculdade de Farmácia, Programa de Pós-Graduação em Ciências Farmacêuticas, Universidade Federal do Rio Grande do Sul, Av. Ipiranga, 2752, Porto Alegre, RS 90610-000, Brazil
e-mail: ruy.beck@ufrgs.br

Introduction

Currently, there is a growing interest in the study of antioxidants [1, 2]. Recent discoveries have pointed out the effects of free radicals in the body, which are involved in energy production, phagocytosis, and regulation of cell growth among others [3]. Oxidative stress is a condition that occurs in a system when the generation of reactive oxygen species exceeds the capacity of neutralization and disposal system. The instability may result from a lack of antioxidant capacity caused by disturbances in the production, distribution, or by an abundance of reactive oxygen species from endogenous sources or stressful environmental conditions. Oxidative stress has been implicated in a growing list of diseases such as cardiovascular and neurodegenerative diseases, cancer, arthritis, hemorrhagic shock, cataracts, as well as in aging processes [3–5].

Among the various classes of antioxidants, naturally occurring phenolic compounds have received much attention in recent years due to their inhibition of lipid peroxidation and lipoxygenase [4]. The antioxidant activity of phenolic compounds is mainly related to their reducing properties and chemical structure [6]. These characteristics play an important role in the neutralization or sequestration

of free radicals and chelation of transition metals, acting both in the initiation step and in the propagation of oxidation [6]. The intermediate species formed by the action of antioxidant phenolic compounds are relatively stable due to the resonance of the aromatic ring in their structure [7].

Natural flavonoids are phenolic compounds known for their significant scavenging properties on oxygen radicals both in vivo and in vitro [8, 9]. Many studies have showed the importance of their antiradical activity [10–13]. Moreover, their actions in humans have been subject of extensive research, and natural flavonoids have been described to possess several biological activities such as antioxidant, anti-inflammatory, antitumor, and antiviral properties [14].

Rutin (quercetin-3-O-rutinoside), the glycoside of quercetin, is abundantly found and distributed in plants such as in buckwheat seed, fruits, and fruit rinds, especially citrus fruits (orange, grapefruit, lemon). It presents important properties in human health like its significant scavenging properties on oxidizing species such as hydroxyl radical, superoxide radical, and peroxyl radical [15], as shown by many in vitro and in vivo experiments [16–18]. Furthermore, rutin has several pharmacological activities including anti-allergic, anti-inflammatory, and vasoactive properties [15, 19, 20]. Rutin offers an advantage over other flavonoids, which in some occasions behave as pro-oxidant agents and catalyze oxygen production [15]. Therefore, it is considered a non-toxic molecule and not oxidized. On the other hand, the main disadvantage of the molecule is its poor solubility in aqueous media, explaining its poor oral or topical bioavailability [19] and being a drawback to its conversion in adequate dosage forms.

In the last decade, an alternative drug delivery approach was developed to overcome the poor water solubility of rutin by reducing its particle size [19]. A decrease in the drug particle size leads to an increase in the saturation solubility, to an enlarged surface area and to a higher dissolution velocity [21]. Formulating rutin as drug nanocrystals has significant importance to improve its physicochemical properties, especially its oral bioavailability. Some studies have shown techniques for lyophilization and spray drying nanocrystals of rutin in order to ensure their redispersibility as separate and non-aggregated particles. This characteristic is a critical point to improve the dissolution behavior of drugs, especially from a tablet dosage form [19, 20].

On the other hand, polymeric nanoparticles have been designed to encapsulate lipophilic drugs not only to improve their physicochemical properties but also to target organs or tissues, to avoid drug degradation, to improve drug efficacy, and to circumvent drug toxicity [22]. Nanocapsules are polymeric nanoparticles composed of an oily core surrounded by a polymeric wall stabilized by surfactants at the particle/water interface [23]. The potential use of nanocapsules includes the protection of drugs against inactivation in the gastrointestinal tract [21], delivery of poorly water-soluble compounds [24, 25], and protection of sensitive materials to chemical degradation induced by UV light [26–28]. As the polymeric nanoparticles, nanoemulsions have been also investigated as drug delivery systems in the last years [29–32]. These colloidal systems are composed of oily nanodroplets stabilized by surfactants in an aqueous medium.

All these considerations into account, the main objective of our study was to develop aqueous rutin delivery systems and to evaluate the influence of the association of rutin to different nanostructures (nanocapsules and nanoemulsions) on its in vitro antioxidant activity and UV photostability. Nanocapsules and nanoemulsions were compared to establish the importance of the polymeric layer around the nanodroplets by means of a systematic physicochemical characterization of both formulations. The development of such formulations aimed to obtain aqueous systems containing rutin, as an intermediate or final pharmaceutical product. To the best of our knowledge, no report on the association of rutin to polymeric nanocapsules is currently available in the scientific literature. The administration of flavonoids by means of nanovectors may be useful for the development of advanced delivery systems for these powerful compounds, in view of their adoption in primary and secondary disease prevention, either for oral or parenteral administration [33].

Materials and Methods

Materials

Rutin, poly-(ε-caprolactone) (PCL), and sorbitan monostearate (Span 60®) were acquired from Sigma–Aldrich (São Paulo, Brazil). Polysorbate 80 (Tween 80®) was supplied by Henrifarma (São Paulo, Brazil). Grape seed oil was obtained from Dellaware (Porto Alegre, Brazil). All other chemicals and solvents presented pharmaceutical or HPLC grade and were used as received.

Preparation of Nanoparticles

Rutin-loaded nanocapsule suspensions (R-NC) and nanoemulsions (R-NE) were prepared in triplicate ($n = 3$) by the interfacial deposition of preformed polymer method and spontaneous emulsification, respectively [34, 35]. For the preparation of nanocapsules, an organic solution containing the grape seed oil (3.3 ml), sorbitan monostearate (0.776 g), the polymer (1.0 g), and acetone (147 ml) was

subjected to magnetic stirring, at a temperature of 40°C. After 1 h, an ethanolic solution containing the rutin (120 ml) was added to this organic phase maintaining the agitation for a further 10 min. Then, the organic phase was injected into an aqueous phase (534 ml) containing Tween 80® (0.776 g). Acetone was removed and the aqueous phase concentrated to 100 ml by evaporation at 40°C under reduced pressure reaching a final concentration of 0.25 mg ml^{-1} of rutin. All formulations were stored at room temperature and protected from light (amber glass flasks). Nanoemulsions were prepared using the same experimental conditions, but omitting the presence of the polymer in the organic phase. In addition, in order to evaluate the influence of rutin in the physicochemical characteristics of such nanostructures, blank formulations (placebo) were prepared similarly, but omitting the presence of rutin. These formulations were called B-NC and B-NE, for blank nanocapsules and blank nanoemulsions, respectively. Table 1 summarizes the abbreviation presented in Tables and Figures.

Characterization of Nanoparticles

Rutin Content

Rutin was assayed by liquid chromatography (LC). The chromatographic system consisted of a Gemini RP-18 column (150 × 4.60 mm, 5 μm, Phenomenex, Torrance, USA) and a Shimadzu instrument (LC-10AVP Pump, UV–VIS SPD-10AVP Module, Class-VP Software, Shimadzu, Tokyo, Japan). The mobile phase consisted of methanol/water (50:50% v/v) acidified with phosphoric acid (apparent pH 4.0) pumped at a flow rate of 1.0 ml min^{-1}. The volume injected was 20 μl, and rutin was detected at 352 nm. Rutin content (mg ml^{-1}) was determined ($n = 3$) after its extraction with methanol from nanocapsules or nanoemulsions (1.6 ml of the formulation to 10 ml of methanol) and dilution with the mobile phase to a concentration of 20 μg ml^{-1}. Validation of the LC assay demonstrated that this method was linear ($y = 30{,}322\times - 6{,}233.7$, $r = 0.9999$, $n = 5$) in the range of 5–30 μg ml^{-1}, precise (RSD: 1.86% for repeatability and 0.70% for intermediate precision) and accurate (RSD: 1.70%). The specificity was tested in presence of the nanoparticle adjuvants and demonstrated that they did not alter the rutin assay [36].

Encapsulation Efficiency

Free rutin was determined in the ultrafiltrate after separation of the nanoparticles by ultrafiltration/centrifugation technique (Microcon 10,000 MW, Millipore). Encapsulation efficiency (%) was calculated by the difference between the total and free rutin concentrations determined in the nanoparticles (drug content) and in the ultrafiltrate, respectively, using the LC method previously described.

pH Measurements

The pH values of formulations were determined by immersion of the electrode directly in the dispersions using a calibrated potentiometer (MPA-210 Model, MS-Tecnopon, São Paulo, Brazil), at room temperature.

Particle Size Analysis, Polydispersity Indices, and Zeta Potential

Particle sizes and polydispersity indices ($n = 3$) were measured by photon correlation spectroscopy after adequate dilution of an aliquot of the suspension in reverse osmosis water (Brookhaven Instruments Corporation, USA). The zeta potentials were determined after dilution of the samples in 10 mM NaCl aqueous solution (Brookhaven Instruments Corporation, Holtsville, USA).

Table 1 List of nomenclatures presented in tables and figures

Abbreviation	Meaning
B-NC	Blank nanocapsules (nanocapsules prepared without drug)
R-NC	Rutin-loaded nanocapsules
B-NE	Blank nanoemulsion (nanoemulsion prepared without drug)
R-NE	Rutin-loaded nanoemulsion
R-SE	Rutin ethanolic solution
k	Release rate constant according (monoexponential kinetic)
k_1	Release rate constant of the burst phase (biexponential kinetic)
k_2	Release rate constant of the sustained phase (biexponential kinetic)
a	Initial concentration of rutin at the burst phase (biexponential kinetic)
b	Initial concentration of rutin at the sustained phase (biexponential kinetic)
r	Regression coefficient
MSC	Model selection criteria

Morphological Analyses

Morphological analyses were conducted at Centro de Microscopia (UFRGS, Brazil) by transmission electron microscopy (TEM; Jeol, JEM 1200 Exll, Japan) operating at 80 kV. Diluted suspensions and nanoemulsions were deposited on specimen grid (Formvar-Carbon support films, Electron Microscopy Sciences), negatively stained with uranyl acetate solution (2% w/v) [37] and observed at different magnifications.

Antioxidant Activity and Photostability Study

The system for the irradiation of the samples was developed by Carvalho et al. [38] and consisted of a 400 W high-pressure mercury lamp (Silvania) as UV radiation source, a cooling system based on air and water circulation, a thermo-regulator for the temperature control, a holder for 12 quartz tubes, and an aluminum-based block. In quartz tubes, 10 ml of each sample (R-NC, R-NE and a rutin ethanolic solution—R-ES) was placed and exposed to UV radiation for 30 min ($n = 3$). Every 5 min, samples were taken from the tubes and analyzed by LC to determine the content of rutin. In order to determine the antioxidant activity, 40 µl H_2O_2 was added to the sample before starting the irradiation process. The amount of H_2O_2 was added in excess, since the concentration of H_2O_2 is 10 times the concentration of the sample and the lamp has a limiting quantum yield for the photolysis of H_2O_2. The artificial generation of the hydroxyl radical was carried out by the decomposition of H_2O_2 in the presence of UV radiation (Eq. 1):

$$H_2O_2 + hv \rightarrow 2 \cdot OH \quad (1)$$

The kinetic constant for the reaction of rutin with the ·OH radical was determined by subtracting the contribution of direct photolysis of rutin from the ·OH radical reaction kinetic constant, according to the following equation (Eq. 2):

$$k_{OH+hv} - k_{hv} = k_{OH} \quad (2)$$

where $k_{OH + hv}$ represents the kinetic constant determined by the rutin decay after UV photolysis in the presence of H_2O_2, k_{hv} represents the kinetic constant determined by the direct photolysis of rutin in absence of H_2O_2, and k_{OH} represents the liquid free radical reaction kinetic constant of the ·OH radical with the antioxidant.

In Vitro Rutin Release Assay

In vitro drug release profiles from rutin-loaded nanostructures were evaluated (n = 3) by the dialysis bag method, using water/ethanol (65:35 v/v) as medium, at 37°C [39]. The dialysis bag (Spectra Por 7, 10 Kd, Biosystems) containing 1 ml of the sample (0.25 mg ml^{-1}) was put into a glass test-tube containing 200 ml of dissolution medium. This system was maintained under constant moderate stirring during all the time. The withdrawal of 2 ml of the external medium from the system was done at predetermined time interval, replaced by an equal volume of fresh medium, and filtered through a 0.45-µm membrane. Rutin was assayed in the samples by LC according to the method previously described. However, the injection sample volume was increased to 100 µl to allow the assay of rutin at lower concentrations. This LC method was validated according to the following characteristics: linearity ($y = 167{,}806\times + 1{,}170.3$, $n = 3$, $r = 0.9997$), concentration range (0.1–2.0 mg ml^{-1}), and precision (RSD: 0.90%).

In order to obtain a better understanding of the influence of the type of nanoparticle structure on the rutin release behavior, the mathematical modeling (MicroMath® Scientist® for Windows) was used to analyze the drug release profiles. Monoexponential ($C = C_0e^{-kt}$) and biexponential ($C = ae^{-k_1t} + be^{-k_2t}$) models were used to evaluate the rutin release profiles. The release rate constants are k, k_1, and k_2 and the initial concentration of rutin are C_0, a, and b. The selection of the model that best fit the release profiles was based on the best correlation coefficient, the best model selection criteria (MSC), both provided by the software and the best graphic adjustment. The meaning of all these abbreviations is presented in Table 1.

Statistical Analysis

Formulations were prepared and analyzed in triplicate. Results are expressed as mean ± SD (standard deviation). Two-way analysis of variance (ANOVA) was employed in the comparison of the experimental data. Post hoc multiple comparisons were done by Tukey's test for significance at p–values ≤ 0.05. All analyses were run using the SigmaStat Statistical Program (Version 3.0, Jandel Scientific, USA).

Results and Discussion

Preparation and Physicochemical Characterization of Aqueous Nanostructured Systems

All formulations appeared macroscopically homogeneous and their aspects were similar to a milky bluish opalescent fluid (Tyndall effect). The physicochemical characteristics of the formulations are presented in Tables 2 and 3. As can be seen, the formulations presented drug content close to their theoretical value (0.24 and 0.25 mg ml^{-1}), mean

Table 2 Drug content, encapsulation efficiency, and pH of rutin-loaded nanocapsules (R-NC) and rutin-loaded nanoemulsion (R-NE) as well as their respective blank formulations (B-NC and B-NE) ($n = 3$)

Formulation	Drug content (mg ml^{-1})	Encapsulation efficiency (%)	pH
B-NC	–	–	5.79 ± 0.03
R-NC	0.25 ± 0.01	93.33 ± 0.63	5.69 ± 0.08
B-NE	–	–	5.94 ± 0.10
R-NE	0.24 ± 0.01	93.83 ± 0.41	5.59 ± 0.01

– Not applicable

Table 3 Particle size, polydispersity index, and zeta potential of rutin-loaded nanocapsules (R-NC) and rutin-loaded nanoemulsion (R-NE) as well as their respective blank formulations (B-NC and B-NE) ($n = 3$)

Formulation	Particle size (nm)	Polydispersity index	Zeta potential (mV)
B-NC	120.37 ± 2.44	0.11 ± 0.06	−20.55 ± 3.63
R-NC	124.30 ± 2.06	0.12 ± 0.02	−27.12 ± 9.19
B-NE	128.06 ± 3.38	0.13 ± 0.03	−26.03 ± 2.27
R-NE	124.17 ± 1.79	0.10 ± 0.02	−26.92 ± 1.45

particle size in the nanometric range (122–126 nm), acidic pH, and negative zeta potential (between −26.0 and −27.0 mV). Polydispersity indices below 0.20 indicated an adequate homogeneity of these systems [26]. In addition, neither the presence of rutin nor the presence of the polymer influenced the physicochemical characteristics of the structures. Moreover, nanocapsules and droplets of the nanoemulsions were spherical in shape as showed by the images obtained by transmission electron microscopy (Fig. 1). Although the type of the nanostructured system did not show any influence on the physicochemical characteristics, the morphological analyses by TEM revealed that rutin-loaded nanoemulsions (R-NE) presented rutin nanocrystals around the droplets when compared to its respective blank formulation (B-NE). Rutin nanocrystals were not observed in nanocapsule formulation (R-NC). These results can be explained by the leakage of rutin from nanoemulsion due to the absence of the polymeric layer around the droplets and its subsequent crystallization in the aqueous dispersed medium as previously demonstrated for dexamethasone under storage [37, 40].

Antioxidative Activity, UV Protodegradation, and In Vitro Release Assay

Figure 2 shows the rutin photodegradation obtained for both formulations (R-NC and R-NE), as well as for rutin ethanolic solution (R-ES). The degradation profiles of rutin

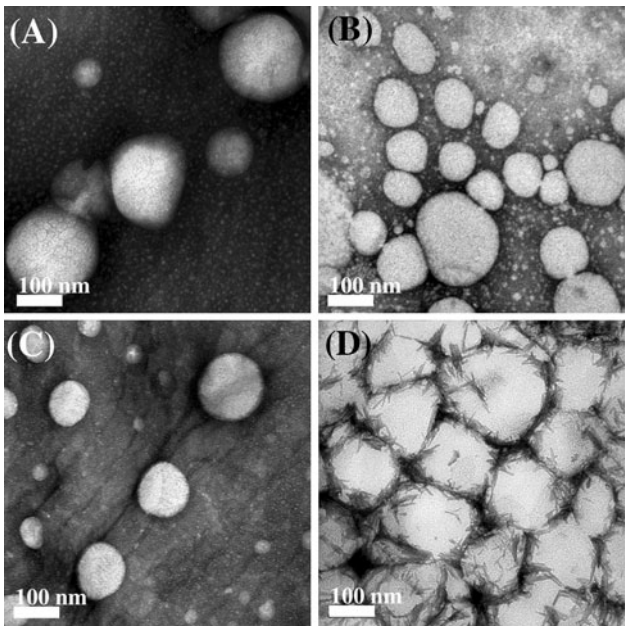

Fig. 1 Transmission electron microscopy images of **a** B-NC, **b** R-NC, **c** B-NE, and **d** R-NE. Bar 100 nm (200,000×)

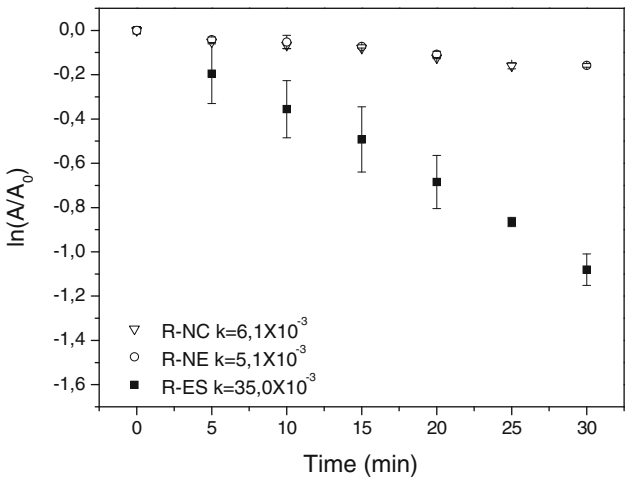

Fig. 2 Photodegradation profile of rutin-loaded nanostructures and rutin ethanolic solution during 30 min of UV irradiation

in the nanostructured formulations (R-NC and R-NE) were according to a first kinetic order, and their respective degradation constants were not significantly different [$k = (6.1 \pm 0.6)\ \ 10^{-3}\ \text{min}^{-1}$, $k = (5.1 \pm 0.4)\ \ 10^{-3}\ \text{min}^{-1}$, respectively] (ANOVA, $p > 0.05$). However, compared to the rutin ethanolic solution [$k = (35.0 \pm 3.7)\ 10^{-3}\ \text{min}^{-1}$], both nanostructured formulations showed a significant lower rutin degradation rate (ANOVA, $p \leq 0.05$). These results showed that the association of rutin to the nanocapsules or nanoemulsions led to an increase of 5.3 and 6.9 times in the rutin photostability, respectively, during the 30 min of exposure to UV radiation.

The antioxidant activity (radical scavenging activity) of rutin was evaluated by adding an amount of H_2O_2 in excess to the samples (before the irradiation) leading to the quantitatively controlled formation of ·OH radicals, which are the most harmful radicals formed under physiological conditions. In this case, the decay kinetics were significantly different among all samples (R-NC, R-NE and R-SE) and according to a first-order kinetics (ANOVA, $p \leq 0.05$). The nanoparticle formulations (R-NC and R-NE) showed decay kinetics about 2.1 and 1.5 times slower than the solution [$k = (19.5 \pm 0.5)\ 10^{-3}\ \text{min}^{-1}$, $k = (26.6 \pm 2.6)\ 10^{-3}\ \text{min}^{-1}$ and $k = (40.1 \pm 1.7)\ 10^{-3}\ \text{min}^{-1}$, for R-NC, R-NE and R-SE, respectively], indicating a prolonged antioxidant activity of rutin, when associated to the nanostructures (Fig. 3). The difference between the decay kinetics of the different nanoparticles (ANOVA, $p \leq 0.05$) could be explained by the presence of rutin nanocrystals adsorbed on the surface of the nanodroplets of nanoemulsions (as observed by TEM—Fig. 1), making rutin more readily accessible to react with the ·OH free radical.

In order to evaluate if the rutin release rate from the different nanoparticles could also play an important role in this different antioxidant behavior we carried out an in vitro drug release experiment using the dialysis bag technique. Figure 4 shows the in vitro drug release profiles from rutin-loaded nanocapsules (R-NC) and rutin-loaded nanoemulsions (R-NE). Both formulations promoted a rapid and similar release of rutin (release close to 100% in 24 h). The release profiles were modeled using the monoexponential and biexponential equations. According to the values of the correlation coefficients and the criterion for model selection (MSC), the data fit better to the biexponential equation (Table 4) for both formulations, showing a burst release at an early stage followed by a sustained phase.

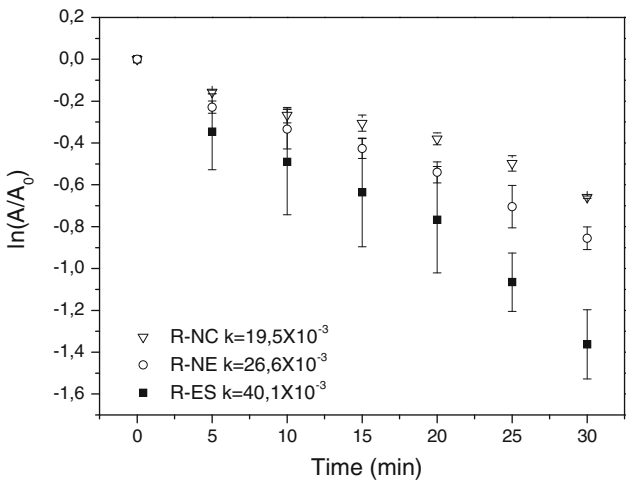

Fig. 3 In vitro antioxidant activity of rutin-loaded nanostructures and ethanolic solution after 30 min of UV irradiation

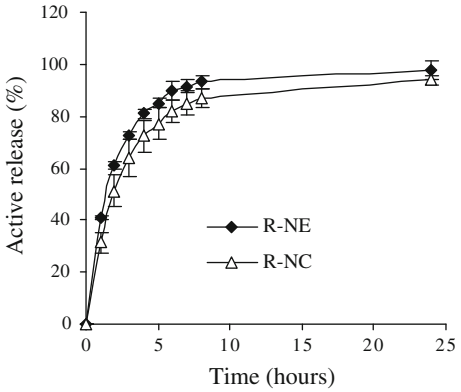

Fig. 4 In vitro rutin release profile from nanocarriers (R-NC and R-NE) using the dialysis bag method ($n = 3$).The lines correspond to the fitting to the biexponential equation

Table 4 Rate constants, correlation coefficients, and MSC obtained by the mathematical modeling of drug release data from the different nanocarriers (R-NC and R-NE)

	R-NC	R-NE
Monoexponential		
k (h^{-1})	0.3215 ± 0.0674	0.4336 ± 0.0242
r (range)	0.9979 ± 0.0010	0.9983 ± 0.0016
MSC (range)	2.9935 ± 0.2326	3.0585 ± 0.9828
Biexponential		
k_1 (h^{-1})	0.4113 ± 0.0765	0.8164 ± 0.6039
k_2 (h^{-1})	0.0310 ± 0.0163	0.1393 ± 0.1993
a (mg ml^{-1})	0.8447 ± 0.0597	0.6107 ± 0.3337
b (mg ml^{-1})	0.1285 ± 0.0370	0.3201 ± 0.4125
r (range)	0.9997 ± 0.0002	0.9994 ± 0.0006
MSC (range)	6.5420 ± 0.5612	6.0185 ± 0.8945

The rate constants for the burst phase (k_1) were $0.4113 \pm 0.0765\ h^{-1}$ (R-NC) and $0.8164 \pm 0.6039\ h^{-1}$ (R-NE) and for the sustained phase the rate constants (k_2) were 0.0310 ± 0.0163 (R-NC) and $0.1393 \pm 0.1993\ h^{-1}$ (R-NE). For both phases, R-NC showed lower rate constants compared to R-NE. The percentage of rutin related the burst phase (a) for nanocapsules and nanoemulsions was about 85 and 65%, respectively. On the other hand, the percentage related to the sustained phase was about 13% for R-NC and 32% for the R-NE. Such values showed that rutin is about 60–80% adsorbed on the surface of nanostructures [41, 42], suggesting that the radical scavenging property of rutin against the ·OH radical occurred mostly at the interface particle/water. However, the influence of the drug release from the inner compartment of the nanocarriers cannot be discarded, considering the slower drug

release rate from R-NC at both release phases. This hypothesis can be reinforced by the analysis of the release half-life of rutin, calculated according to the biexponential model. R-NC showed higher values (1.7 and 22 h for the burst and sustained phase, respectively) compared to R-NE (0.8 and 5 h for the burst and sustained phase, respectively). This faster drug release from R-NE can be explained by the absence of the polymer around the oily droplets as well as by the presence of nanocrystals on their surface, as observed by TEM.

Conclusions

This study showed for the first time the development of rutin-loaded nanocapsules and nanoemulsions, as aqueous intermediate or final systems to the development of nanomedicines containing rutin. Both formulations presented an increase in the rutin photostability and a prolonged in vitro antioxidant activity, even if the main mechanism of association of rutin was the adsorption on the particle/droplet surface, as determined by the mathematical modeling of drug release data. Moreover, the presence of polymer did not show any significant influence in the increase of rutin photostability. However, its presence in nanocapsules led to a slower release rate and to a prolonged antioxidant activity against the strongly reactive ·OH radicals compared to the rutin-loaded nanoemulsions. The results showed that such nanostructured systems are a potential alternative to the preparation of rutin delivery systems to treat different diseases related to oxidative stress, including aging processes caused by the action of free radicals.

Acknowledgments JSA thanks CAPES/Brazil for the fellowship. We thank Rede Nanocosméticos CNPq/MCT/Brazil, PRONEX/FAPERGS/CNPq, CAPES and CNPq for the financial support received as well as M.B. da Rosa for his contribution in this work.

References

1. C.M.M. Sousa, H. Rocha e Silva, G.M. Vieira Jr., M.C.C. Ayres, C.L.S. Costa, D.S. Araújo, L.C.D. Cavalcante, E.D.S. Barros, P.B.M. Araújo, M.S. Brandão, M.H. Chaves, Quim. Nova **30**, 351 (2007)
2. A.S. Darvesh, R.T. Carroll, A. Bishayee, W.J. Geldenhuys, C.J. Van der Schyf, Expert Rev. Neurother. **10**, 729 (2010)
3. A.L.B.S. Barreiros, J.M. David, Quim. Nova **29**, 113 (2006)
4. P. Brenneisen, H. Steinbrenner, H. Sies, Mol. Aspects Med. **26**, 256 (2005)
5. U. Cornelli, Clin. Dermatol. **27**, 175 (2009)
6. A. Michalak, Polish J. Environ. Stud. **15**, 523 (2006)
7. S.S. Chun, D.A. Vatem, Y.T. Lin, K. Shetty, Process Biochem. **40**, 809 (2005)
8. M.J. Abad, P. Bermejo, A. Villar, Gen. Pharmacol. **26**, 815 (1995)
9. C. La Casa, I. Villegas, C.A. de la Lastra, V. Motilva, M.J. Martín Calero, J. Ethnopharmacol. **71**, 45 (2000)
10. A. Solomon, S. Golubowicz, Z. Yablowicz, M. Bergman, S. Grossman, A. Altmann, Z. Kerem, M.A. Flaishman, J. Agric. Food Chem. **58**, 6660 (2010)
11. K.L. Krishna, K. Mruthunjaya, J.A. Patel, Int. J. Pharmacol. **6**, 72 (2010)
12. O.A. Fawole, S.O. Amoo, A.R. Ndhlala, M.E. Light, J.F. Finnie, J. Van Staden, J. Ethnopharmacol. **127**, 235 (2010)
13. H. Jiang, W.Q. Zhan, X. Liu, S.X. Jiang, Nat. Prod. Res. **22**, 1650 (2008)
14. J. Yang, J. Guo, J. Yuan, LWT **41**, 1066 (2008)
15. M.L. Calabrò, S. Tommasini, P. Donato, R. Stancanelli, D. Raneri, S. Catania, C. Costa, V. Villari, P. Ficarra, R. Ficarra, J. Pharm. Biomed. Anal. **36**, 1019 (2005)
16. A. Korkmaz, D. Kolankaya, J. Surg. Res. (2009). doi: 10.1016/j.jss.2009.03.022
17. A.R. Verma, M. Vijayakumar, C.S. Mathela, C.V. Rao, Food Chem. Toxicol. **47**, 2196 (2009)
18. S. Itagaki, J. Oikawa, J. Ogura, M. Kobayashi, T. Hirano, K. Iseki, Food Chem. **118**, 426 (2010)
19. R. Mauludin, R.H. Müller, C.M. Keck, Int. J. Pharm. **370**, 202 (2009)
20. R. Mauludin, R.H. Müller, C.M. Keck, Eur. J. Pharm. Sci. **36**, 502 (2009)
21. P. Couvreur, G. Barrat, E. Fattal, P. Legrand, C. Vauthier, Ther. Drug Carrier Syst. **19**, 99 (2002)
22. C.E. Mora-Huertas, H. Fessi, A. Elaissari, Int. J. Pharm. **385**, 113 (2010)
23. A.R. Pohlmann, V. Weiss, O. Mertins, N.P. da Silveira, S.S. Guterres, Eur. J. Pharm. Sci. **16**, 305 (2002)
24. J.M. Fachinetto, A.F. Ourique, G. Lubini, S.B. Tedesco, A.C.F. Silva, R.C.R. Beck, Lat. Am. J. Pharm. **27**, 668 (2008)
25. M. Teixeira, M.J. Alonso, M.M.M. Pinto, C.M. Barbosa, Eur. J. Pharm. Biopharm. **59**, 491 (2005)
26. A.F. Ourique, A.R. Pohlmann, S.S. Guterres, R.C.R. Beck, Int. J. Pharm. **352**, 1 (2008)
27. J.S. Almeida, L. Jezur, M.C. Fontana, K. Paese, C.B. Silva, A.R. Pohlmann, S.S. Guterres, R.C.R. Beck, Lat. Am. J. Pharm. **28**, 168 (2009)
28. M.C. Fontana, K. Coradini, S.S. Guterres, A.R. Pohlmann, R.C.R. Beck, J. Nanosci. Nanotechnol. **10**, 3091 (2010)
29. S.R. Schaffazick, L.L. Freitas, A.R. Pohlmann, S.S. Guterres, Quim. Nova **25**, 726 (2003)
30. S.S. Guterres, M.P. Alves, A.R. Pohlmann, Drug Target Insights **2**, 147 (2007)
31. A.R. Pohlmann, G. Mezzalira, C. De, G. Venturini, L. Cruz, A. Bernardi, E. Jäger, A.M.O. Battastini, N.P. da Silveira, S.S. Guterres, Int. J. Pharm. **359**, 288 (2008)
32. L. Mei, Y. Zhang, Y. Zheng, G. Tian, C. Song, D. Yang, H. Chen, H. Sun, Y. Tian, K. Liu, Z. Li, L. Huang, Nanoscale Res. Lett. **4**, 1530 (2009)
33. G. Leonarduzzi, G. Testa, B. Sottero, P. Gamba, G. Poli, Curr. Med. Chem. **17**, 74 (2010)
34. H. Fessi, F. Puisieux, J.-P. Devissaguet, European Patent 0274961 Al (1988)
35. É. Martini, E. Carvalho, H. Teixeira, Quim. Nova **30**, 930 (2007)
36. ICH – International Conference on Harmonisation of Technical Requirements for Registration of Pharmaceuticals for Human Use: Gudeline on Validation of Analytical Procedure Q2 (R1): Text and Methodology (2005)

37. R.C.R. Beck, S.S. Guterres, J.A.B. Funck, R.J. Freddo, C.B. Michalowski, I. Barcellos, Acta Farm. Bonaer. **22**, 11 (2003)
38. L.M. Carvalho, C. Spengler, J.C. Garmatz, P.C. Nascimento, D. Bohrer, L. Del-Fabro, G. Radis, A.A. Bolli, A.M. Moro, S.C. Garcia, M.B. Rosa, Quim. Nova **31**, 1336 (2008)
39. H. Li, X. Zhao, Y. Ma, G. Zhai, L. Li, H. Lou, J. Control. Release **133**, 238 (2009)
40. R.B. Friedrich, M.C. Fontana, A.R. Pohlmann, S.S. Guterres, R.C.R. Beck, Quim. Nova **31**, 1131 (2008)
41. L. Cruz, L.U. Soares, T. Dalla Costa, G. Mezzalira, N.P. Silveira, S.S. Guterres, A.R. Pohlmann, Int. J. Pharm. **313**, 198 (2006)
42. M.C. Fontana, K. Coradini, S.S. Guterres, A.R. Pohlmann, R.C.R. Beck, J. Biomedi. Nanotechnol. **5**, 254 (2009)